University of Science and Technology of Hanoi

Cosmic ray muons for imaging the hidden structure

Group Project Final Report

Author:
Nguyen Hoang Dang Khoa
Ton That Minh Bao
Nguyen Hoang Long
Do Minh Nghia

Supervisors:
Dr. Cao Van Son
Asc. Prof. Nguyen Thi Hong Van

February 28, 2021

1 Introduction

Muons are elementary particles with similar electric charge and and spin to that of electrons, but much more massive ($\approx 200m_e$) and have much shorter lifetime ($\tau \approx 2.19 \times 10^{-6}\, s$). Note that the lifetime of the particle depends on its velocity or momentum as expected from the Theory of Relativity

$$t = \gamma\tau = \left(1 - \frac{v^2}{c^2}\right)^{-1/2} \tau, \tag{1}$$

where τ is the lifetime of the particle in its rest frame, v is the velocity of the particle and t is the lifetime of the particle in the lab frame (our frame). This explains why high energy particles, even with short lifetime can still exist without decaying over a large span of time.

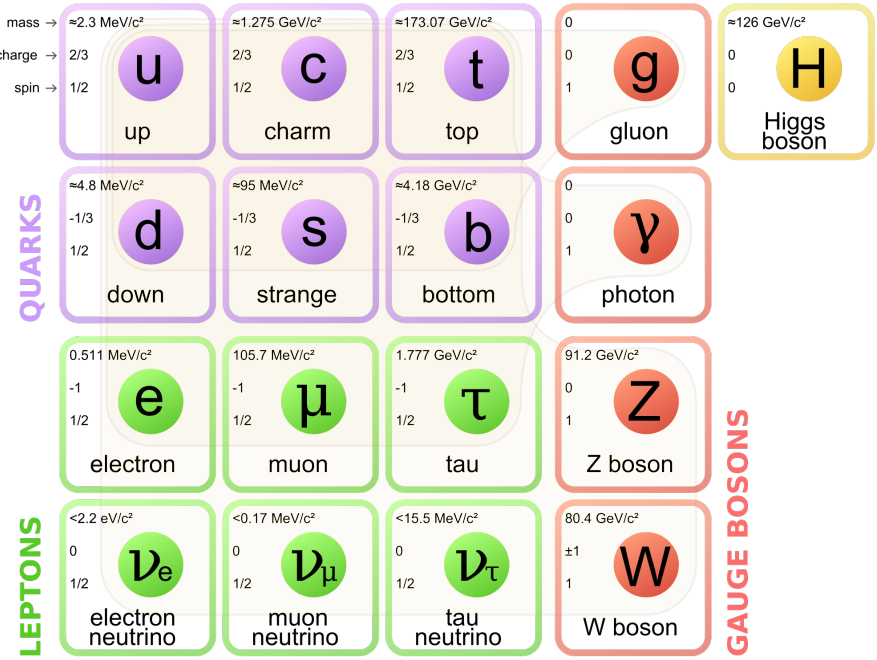

Figure 1: Standard Model of Elementary Particles. There are 6 flavors of quarks and 6 flavors of leptons, along with 4 gauge bosons and Higgs boson. The closed contour in the background grouped the types of particles that interact with each other. Muons (μ) subject to electromagnetic, weak and gravitational interaction. Every quark and lepton has its own anti-particle partner where the associated quantum charge is reversed.

Nearly all muons ($\approx 100\%$) decay into electrons and neutrinos

$$\begin{aligned} \mu^- &\longrightarrow e^- + \bar{\nu}_e + \nu_\mu, \\ \mu^+ &\longrightarrow e^+ + \nu_e + \bar{\nu}_\mu, \end{aligned} \tag{2}$$

where μ^+, e^+ and $\bar{\nu}$ represent anti-muon, positron and anti-neutrino. At the Earth's surface, the majority of muons observed are produced by cosmic rays in the upper atmosphere, these are called *cosmic ray muons*.

Cosmic ray muons are the most numerous high-energy particles at sea-level with intensity $\approx 1\, cm^{-2} \cdot min^{-1}$, which is equivalent to about 50000 muons each minute covered by a typical 4-passenger vehicle, figure 2 shows the vertical fluxes of cosmic rays in the atmosphere with energy greater than $1\, GeV$. They also penetrate much deeper inside materials compared to other particles, figure 3 gives an illustration of how much deeper muon can penetrate compared to others. For those reasons, they can be used as a scanning tool similar to X-ray scanning in order to study properties of a target as in figure 4. This technique is called *muon radiography*, in which it only concern about the fraction of μ passing through the target counted by the

detector. A discovery of an unknown chamber in pyramid were successfully performed using this technique [1].

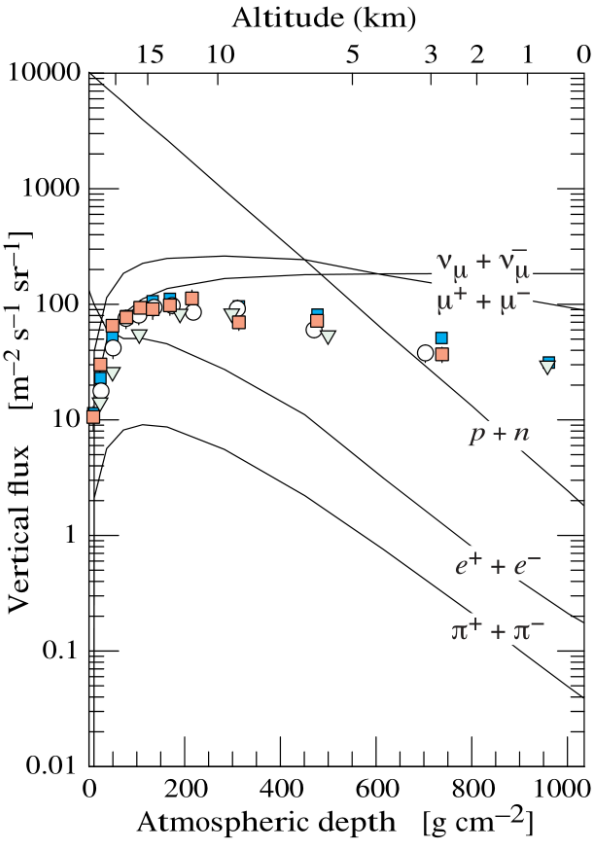

Figure 2: Vertical fluxes of cosmic rays in the atmosphere with $E > 1\,GeV$ [2]. The points show measurements of negative muons with $E > 1\,GeV$ [3–8].

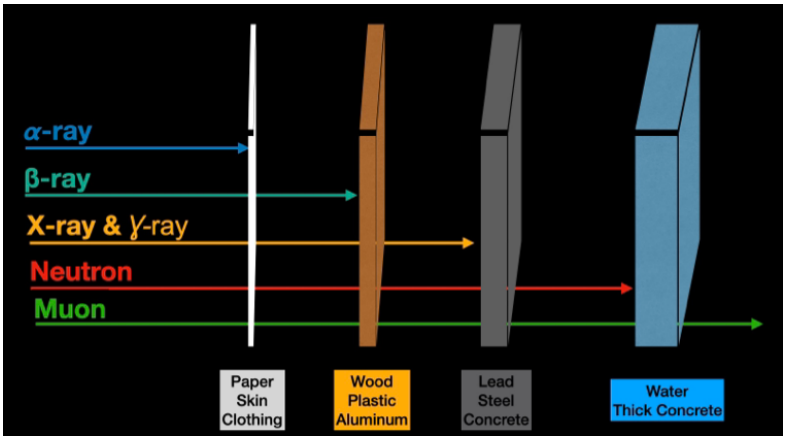

Figure 3: Penetration power of μ compared to different particles.

Another technique using muon is *muon tomography*: this technique makes use of not only the number of muon passing through the target but also their kinematics as well in order to have more informations about the target. However, the scope of this study focuses only on muon radiography.

The purposes of this study are

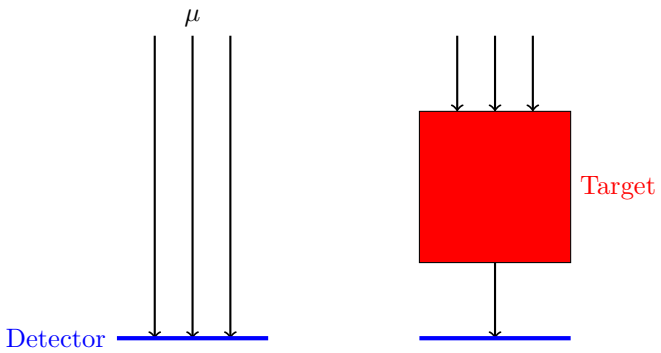

Figure 4: By comparing the muon rate reaching the detector on the left (without object in between) and on the right (with object on the path), one can infer the existence and structure of the object.

- To find a general procedure to theoretically calculate radiography result for arbitrary target
- To simulate radiography results for practical geometries
- To propose an experiment set-up to measure muon using plastic scintillator

2 Theoretical Background

Cosmic ray are highly energetic particles, which consists of mostly proton (p) and alpha (α) particles, these are called *primary cosmic rays*. When these cosmic rays collide with nuclei in the Earth's atmosphere with sufficient energy, *secondary mesons* are created, including pion ($\pi^{\pm}$) and kaon ($K^{\pm}$) particles, which are the source of cosmic ray muons, i.e.

$$\pi^- \longrightarrow \mu^- + \bar{\nu}_\mu, \tag{3}$$
$$\pi^+ \longrightarrow \mu^+ + \nu_\mu, \tag{4}$$
$$K^- \longrightarrow \mu^- + \bar{\nu}_\mu, \tag{5}$$
$$K^+ \longrightarrow \mu^+ + \nu_\mu, \tag{6}$$
$$K^0 \longrightarrow \pi^+ + \pi^-. \tag{7}$$

The deeper inside the material, the more energy muons drop, the term

$$-\frac{dE}{dx} = -\frac{1}{\rho}\frac{dE}{dl} \tag{8}$$

is called the *stopping power* with E being the muon energy, $x = \rho l$ being the *material depth* and ρ being the material density (this quantity can vary in different conditions). If enough energy is lost inside material, μ will be stopped, this is called *ranging out* and also our main concern in this application of radiography since it represents the amount of material on the path way of μ. In general, μ loses energy through 3 main mechanisms

- *Bremsstrahlung radiations*: The Bremsstrahlung radiation is electromagnetic radiation produced when a charged particle is decelerated by another charge particle's electric field. The stopping power of this mechanism is proportional to a quantity defined in (9)

  $$-\frac{dE}{dx} \propto \frac{Z^2 E}{m^2}. \tag{9}$$

  Due to the inverse proportionality with mass, muons emit Bremsstrahlung light nearly 4 orders of magnitude less than $e^{\pm}$.

- *Cherenkov radiations*: The Cherenkov radiation is analogous to the sonic boom, in which the charge particle travel faster than the speed of light *in a medium*. The stopping power in this case follows Frank-Tamm formula (10)

$$-\frac{dE}{dx} = \frac{q^2}{4\pi\rho}\int u(\omega)\omega\left(\frac{1}{\beta^2 n(\omega)} - 1\right) d\omega, \tag{10}$$

with ω being the frequency, $\mu(\omega)$ is the permeability and $n(\omega)$ is the refraction index of the material, $\beta = v/c$ is the velocity of the particle (muon).

- *Ionization*: This refers to when muon transfers energy to electrons inside material, which causes the electrons to be ionized or excited to a higher energy level. The mean stopping power can be illustrated using Bethe-Bloch formula

$$-\left\langle\frac{dE}{dx}\right\rangle = \frac{e^4 Z N_A}{4\pi\epsilon_0^2 m_e c^2 \beta^2 A}\left(\frac{1}{2}\ln\frac{2m_e c^2\beta^2\gamma^2 T_{max}}{I^2} - \beta^2\right) \tag{11}$$

where Z, A are atomic number and molar mass of the material, m_e is the electron mass, I is the *mean excitation* energy of the material

$$I(Z) \approx \begin{cases} 16\,eV \times Z^{0.9}, & Z > 1 \\ 10\,eV \times Z, & Z > 20 \end{cases}$$

and T_{max} is the maximum kinetic energy transfer to *one electron*

$$T_{max} = \frac{2m_e c^2\beta^2\gamma^2}{1 + 2\gamma\frac{m_e}{m_\mu} + \frac{m_e^2}{m_\mu^2}}.$$

Notably, ionization dominates most of the energy dissipated in the range $1 - 1000\,GeV$ as shown in figure 5

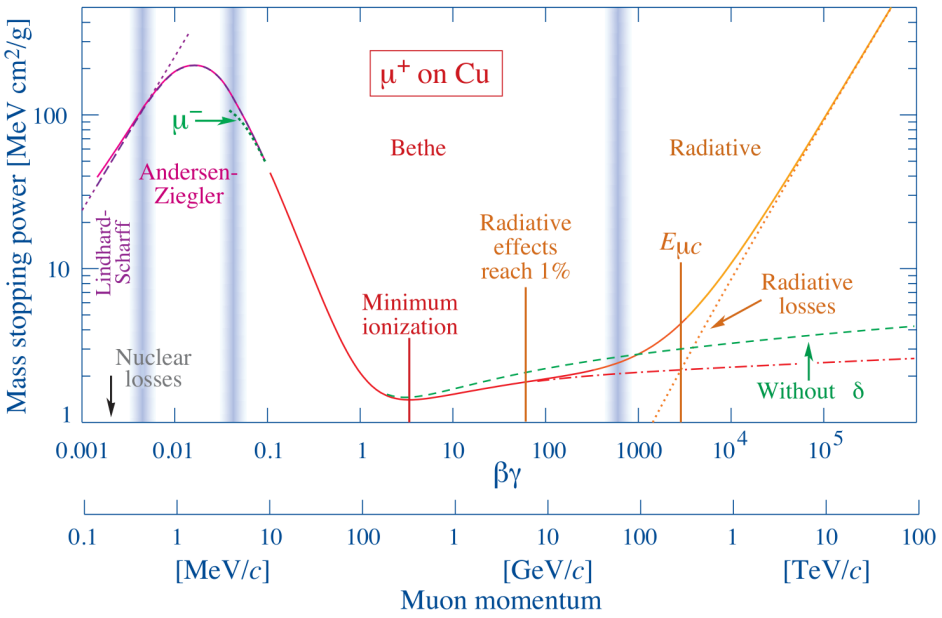

Figure 5: Stopping power of μ^+ in copper as function of muon momentum [2].

So this mechanism alone is a good approximation for the stopping power of muon. For muon with E_μ from $1 - 1000\,GeV$, in concrete (Table 1), we have the approximation

$$-\frac{dE}{dx} \approx 2.1\,MeV \cdot g^{-1} \cdot cm^2 \iff -\frac{dE}{dl} = 2.1 \times \rho = 2.1 \times 2.3 = 4.83\,MeV/cm. \tag{12}$$

The range of μ inside material is approximated as

$$R_\mu(E_\mu) \approx \frac{1}{\rho} \int_{E_\mu}^{m_\mu c^2} \left(\frac{dE}{dx}\right)^{-1} dE, \tag{13}$$

it means that μ with energy E_μ will be stopped by material thicker than $R_\mu(E_\mu)$, e.g. a $4\,GeV$ muon will be penetrate $\approx 7\,m$ in aluminum, or $\approx 2.6\,m$ in iron using this approximation. The range R_μ is also influenced by Multiple Coulomb Scattering (MCS) effect as well, however, since its contribution is small for heavy charged particles like μ, (13) is a good approximation for calculation.

3 Methods

3.1 Theory

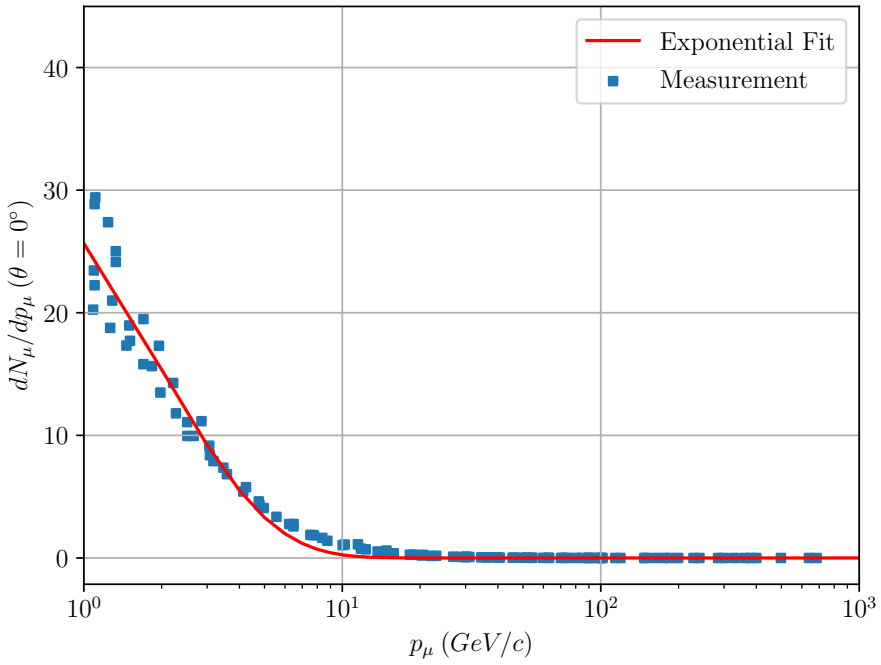

Figure 6: Cosmic μ spectrum at zenith $\theta = 0°$ [2]. The measurement data was digitized from the published plot.

The measurement data of differential spectrum of vertical cosmic muon is fitted using exponential distribution

$$\frac{dN_\mu}{dp_\mu}(p_\mu, \theta = 0°) \approx Ae^{-\lambda(p_\mu - 1\ GeV/c)}. \tag{14}$$

The best-fit result gives $\lambda = 0.5126(GeV/c)^{-1}$ and thus a mean momentum of $\langle p_\mu \rangle = 2.95 GeV/c$. Note that only the data with momentum $p_\mu \geq 1\,GeV/c$ are taken since our plastic scintillator is mostly sensitive with GeV-scale μ.

Normalizing (14) gives the probability density function

$$f_\mu(p_\mu) \approx \lambda e^{-\lambda(p_\mu - 1\ GeV/c)}. \tag{15}$$

If a slab of material has a depth of d along the μ ray's line, we can find the minum energy E_{min} or momentum p_{min} for muon to be able to pass through by solving

$$R_\mu(E_{min}) = d \iff E_{min} \approx d \times \rho \frac{dE}{dx} \approx p_{min} c. \tag{16}$$

The approximation is valid since stopping power in general does not vary much in this energy range. Then the fraction of μ passing through this slab is

$$F(\rho, d) = \int_{p_{min}+1}^{\infty} f_\mu(p_\mu)\, dp_\mu \approx e^{-\lambda p_{min}}, \tag{17}$$

the integral is taken from $p_{min} + 1$ because only the particles with $p > 1\, GeV$ after leaving the material can be detected as our previous assumption. Ideally, the muon distribution is homogenous in space, (16) can be used for any point to obtain a μ fraction map for the whole geometry and thus a map of the amount of material on the μ line of sight.

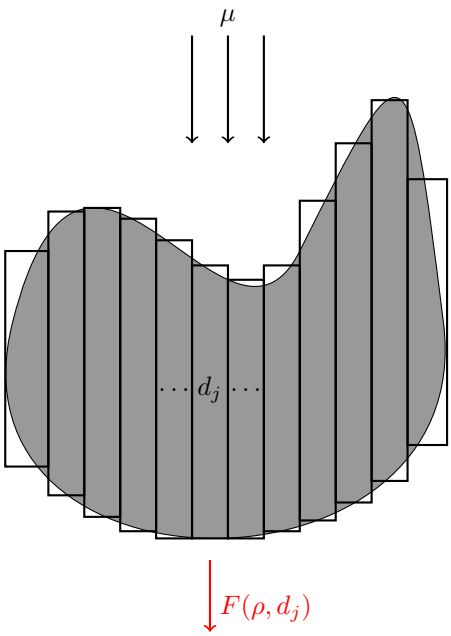

Figure 7: Rough calculation sketch with arbitrary geometry.

In order to test with the simulation, we will use this procedure to calculate the result for a small pyramid with and without 2 empty chambers at the center of the pyramid. The material making up the pyramid will be assumed to be concrete with parameters listed in Table 1

Table 1: Density and mean excitation energy of some materials [9].

	$\rho\ (g \cdot cm^{-3})$	$I\ (eV)$
Concrete	2.3	135.2
Rubber (Natural)	0.92	59.8
Aluminum (Al)	2.699	166
Uranium (U)	18.95	890

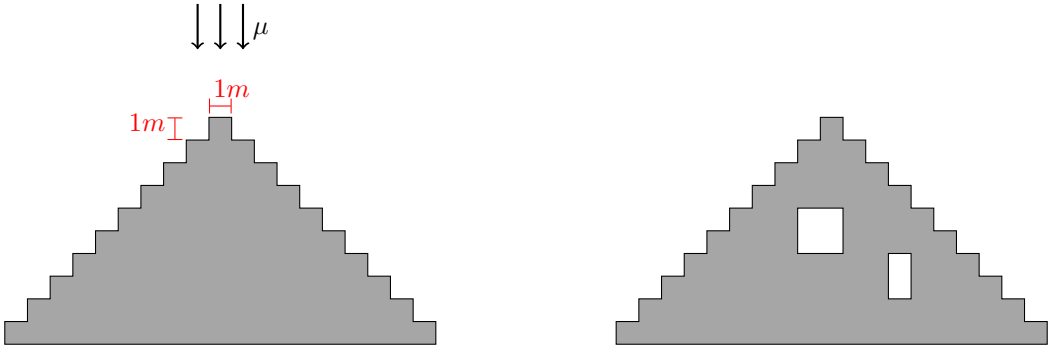

(a) Pyramid model.

(b) Pyramid with 2 empty rooms.

Figure 8: Simple 2D projection of pyramid made of concrete.

3.2 G4beamline Simulation

Many geometries were simulated using G4beamline software. G4beamline is a particle tracking simulation program [10] based on Geant4 [11–13], and is optimized for simulating beamlines. Due to its ability to model the decays and interactions of beam particles, it is capable of simulating highly realistic model and can be adopted for muon tomography and radiography. Some geometries ranging from simple to complex were simulated using the built-in cosmic ray μ profile, namely pyramid and truck.

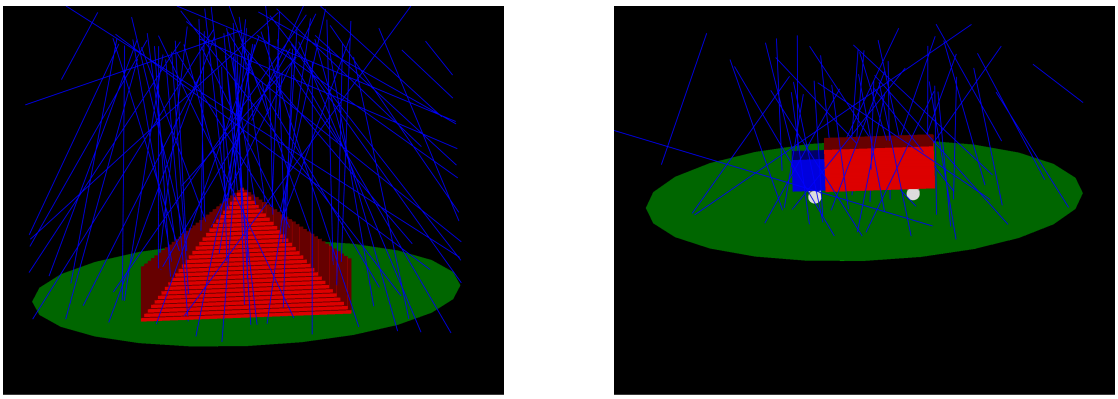

(a) Pyramid model. The structure is made of concrete.

(b) Truck model. The head of the truck is filled with aluminum, the body of the truck is an empty aluminum box and the tires are made of rubber.

Figure 9: Muons passing are blue lines, the circular plate is the ideal virtual detector which can detect every particle in every energy range.

3.3 Muon counter with Plastic Scintillator and MPPC

In order to measure the number of μ, 2 main components were used

- **Multi-Pixel Photon Counter (MPPC):** A photon detector comprised of multiple avalanche diode pixels. The device is a silicon photomultiplier developed by Hamamatsu [14]. This is the third generation MPPC, model S13081-050CS(X1), which has many advantages including high gain, immunity to magnetic field, compact size and simple readout circuit.

- **Plastic Scintillator:** A material that emits photons when interacting with a charged particle. The peak emission of the scintillator is 420 nm, which is in the blue part of visible light. The plastic scintillator we worked with was a bar of dimension $61.1 \times 2.5 \times 1.1\ cm$
- **Wavelength-Shifting fiber:** To shift the wavelength of emitting photons to green light, which is more sensitive by the photosensors and electronics in figure 11 and 12.

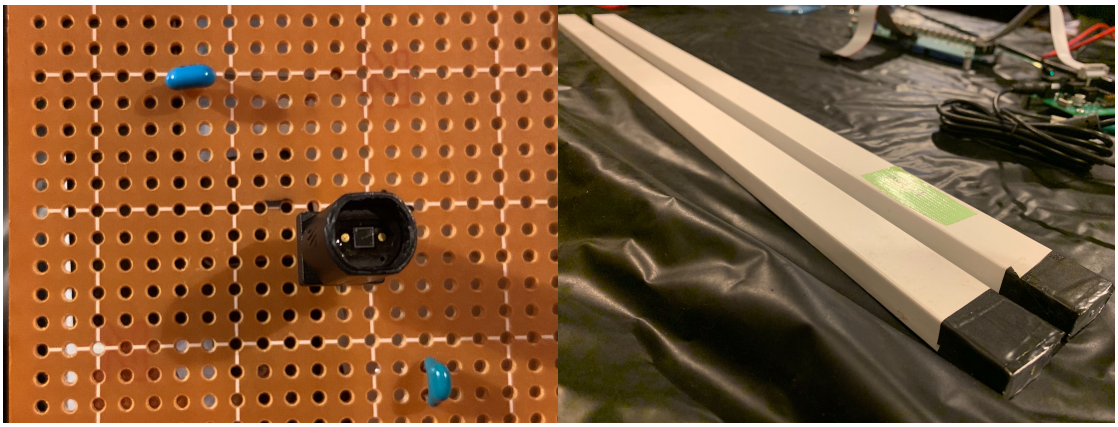

Figure 10: Equipments in ICISE, Quy Nhon: MPPC (left) is mounted on a circuit board and Scintillator (right). To get MPPC signal, an operational voltage need to be provided.

To work with MPPC, investigating its characteristics is needed, i.e. dark count rate, gain, crosstalk, after-pulse, ... Due to time limitation, only the dark count rate of the MPPC was measured during our time in ICISE. Dark count rate is measured while the MPPC is completely covered in nearly no light condition, this procedure is summarized in Figure 11

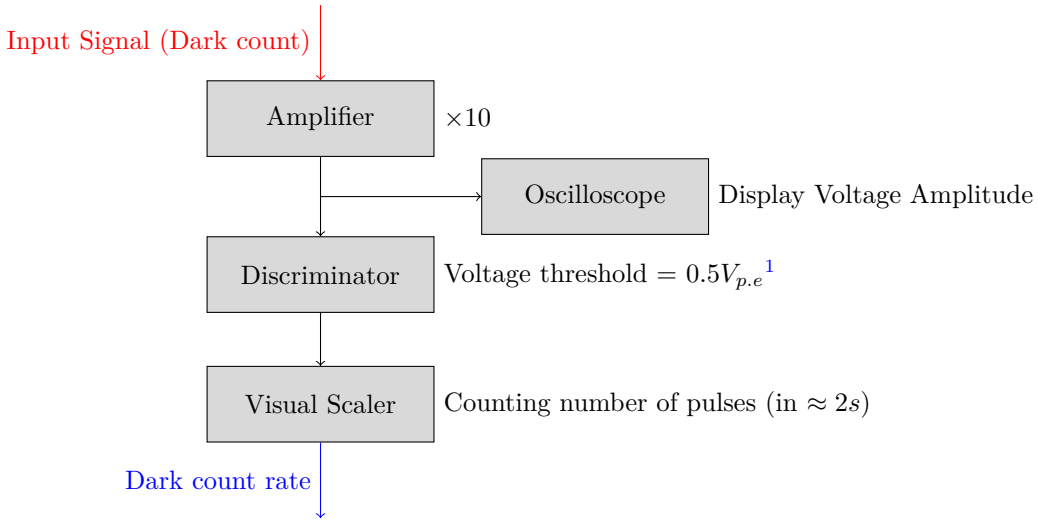

Figure 11: Measuring Dark Count rate procedure.

The measurement is performed 100 times, and is recorded manually. Having the dark count rate, the number of photons induced by one μ were then measured by the procedure as in figure 12. Note that only a fraction of photons emitted were recorded by the MPPC through the wavelength-shifting fiber

[1] p.e stands for "photon equivalent"

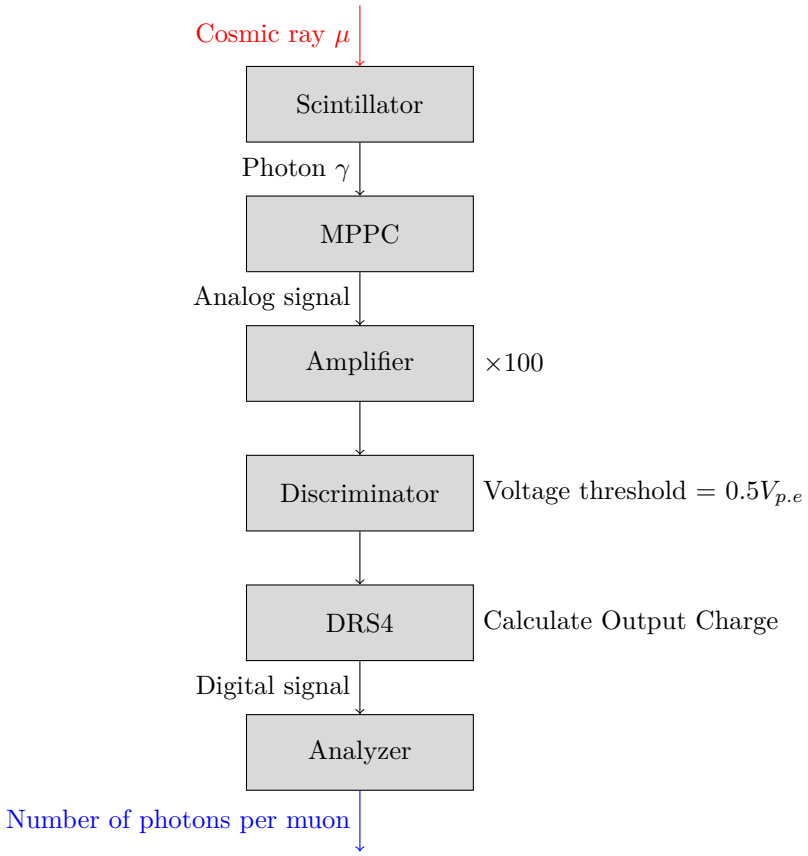

Figure 12: Cosmic muon measurement procedure.

The result of the two measurements are illustrated in section 4. Then by having the number of photon signals per muon, arranging 2 or 3 layers of scintillator, and if a signal similar to a muon occurs in all layers at once, one muon is counted. However, for a bar-shaped scintillator, only the muon signal can be recorded without knowing the position of incident, thus to obtain a 2-dimensional muon counter, many scintillators are needed as in figure 13

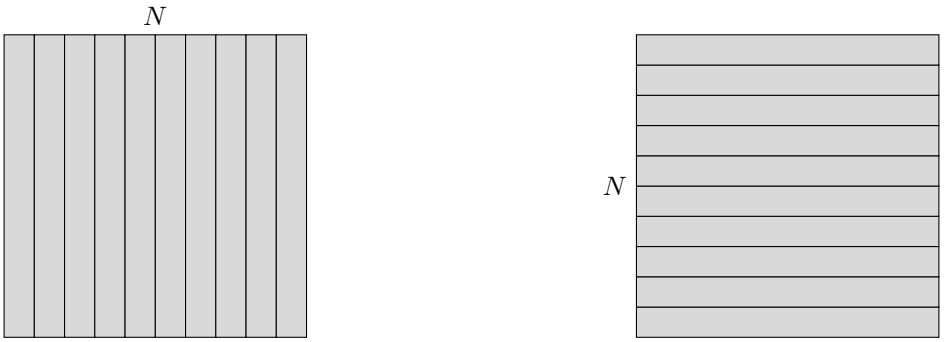

(a) vertical layers. (b) Horizontal layers.

Figure 13: Layers of scintillators.

The set-up consists of overlaying levels of vertical and horizontal structures with plastic scintillator as elements. And by processing individually for each scintillator, we can obtain the number of muon hitting each pixel-like element during a time interval. Multiple layers need to be used to track the trajectory of particles, identify them or measure their momentum (using the range or the gyroradius in known magnetic field).

4 Results

Theoretically, if MCS is not considered and ranging out is the only muon stopping mechanism, investigating the model in figure 8 using (15) gives the result in figure 14.

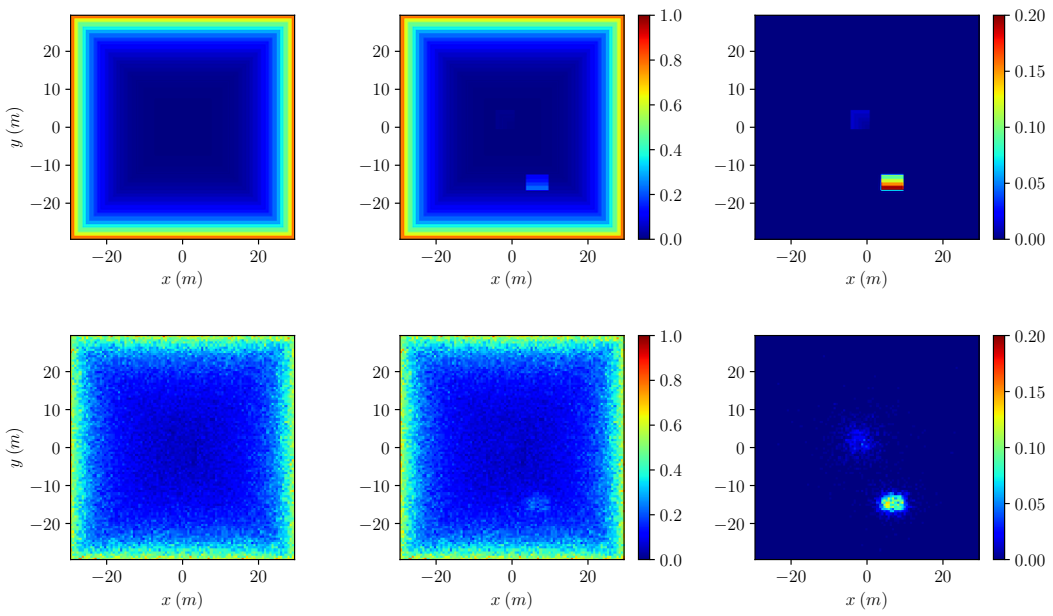

Figure 14: The first row is the theoretical estimation for a fully filled pyramid (left), that with 2 empty chambers (center) and their difference (right). The second row is simulation result from 5 millions cosmic muon events in G4beamline.

The outer parts of the pyramid appear brighter than the inner part near the center. This is due to the geometric property of the pyramid that there is less material in this part. Therefore more muons can pass through this part than they can in the inner part. Compare to the results obtained when there is no room, only one chamber is clearly visible while the other is much fainter. The reason for this is that the fainter chamber is closer to the center of the pyramid, where the amount of material muon has to pass through is much higher, so even with the chamber present, the remaining material is still enough to shield most of the muon in between. Thus we conclude that the functional form f_μ of (15) gives a good estimation for the energy range $1 - 10\,GeV$ since it agrees with the realistic simulation, while for very high energy muons at the inner part, the simulation showed that there are more muon detected than in the calculation. On the other hand, the comparison between an empty truck and a truck with a block of Uranium inside is simulated in Figure 15

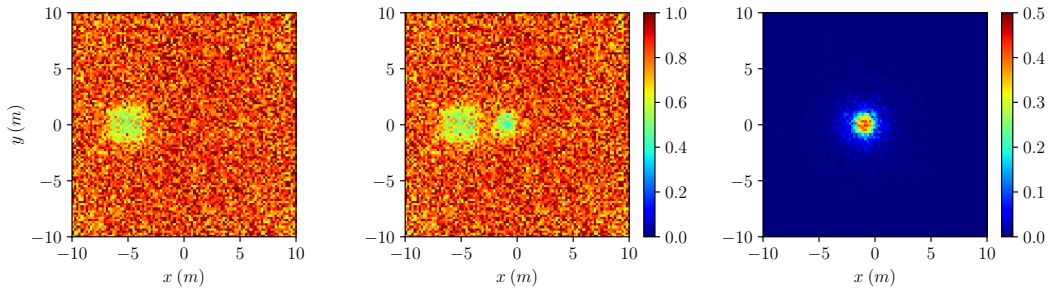

Figure 15: Empty truck (left), truck with Uranium hidden (center) and their difference (right).

In this case, muon kinematics might be used to enhance the image of the inner structure since more details are necessary in meter scale of the truck. The dark count rate of the MPPC was measured statistically as in figure 11 for 100 times, which has the histogram of figure 16

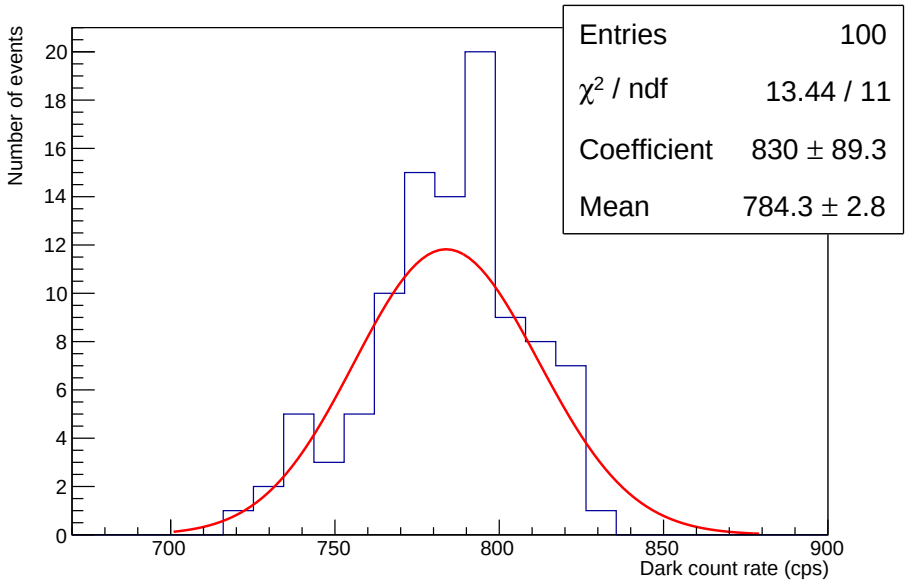

Figure 16: Dark count rate histogram, the red curve is the Gaussian fit.

which yields a dark count rate level of $\mu \pm \sigma \approx 784 \pm 28\, cps$ with 68% confidence. On the other hand, the gain of the MPPC, which is the number of electrons ejected by one photon signal, is measured to be $\approx 2.5 \times 10^7$, this corresponds to an output charge per photon of $\approx 4\, pC$. On the other hand, with the procedure in figure 12, output charge of 191 events (or muon candidates) were recorded and fit with Landau function.

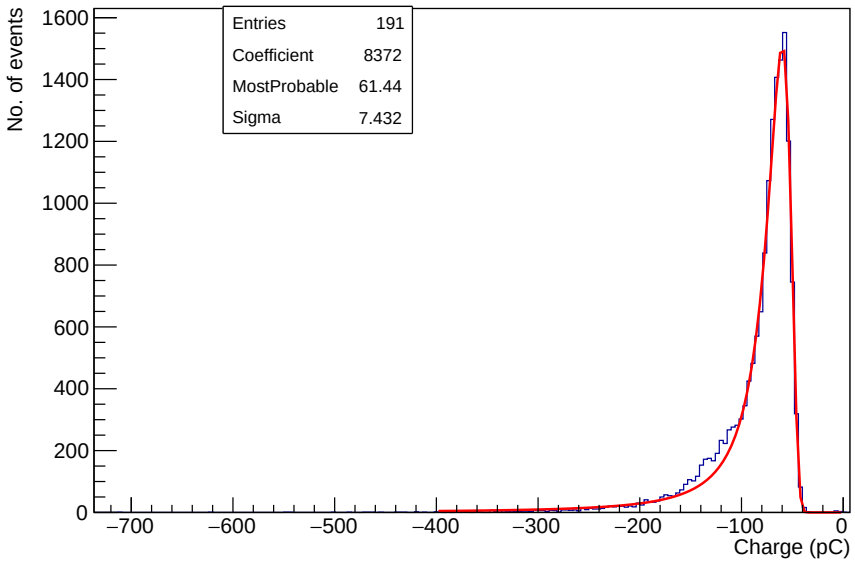

Figure 17: Integrated charge distribution of 191 muon candidates. By dividing this charge to the charge of a single photoelectron, we can calculate how many photons induced by the incoming muon. The red line is the fit using Landau function.

By this result, the most probable output charge is $\approx 61.44 \pm 14\, pC$ and thus the number of photons captured per muon is $\approx 15 \pm 3$ photons. With rough approximation, on the other hand, light yield of scintillator is around ≈ 10000 photons/MeV and the energy loss of μ when passing through the scintillator is $\approx 2\ MeV/cm$. Thus the total number of photons emitted by 1 μ in the scintillator is $\approx 10000 \times 2 \times 1.1 = 22000$ photons where 1.1 cm is the scintillator thickness. In all these photons emitted, roughly about 1% of them manage to get into the wavelength shifting fiber, and only about 30% of these photons can get to the MPPC with an efficiency of 35%. Therefore the expected (raw estimation) number of photon signals per muon is $22000 \times 1\% \times 30\% \times 35\% = 23$, which is reasonable since it is on the same scale with the result measured. Precise calculation has yet to be developed and unfortunately, further experiments have not been executed due to lack of time and budget.

5 Discussion

As shown in the previous section, the simple theoretical calculation gives a good estimation for experimentalists to have an expectation before measuring. However, it is shown to be good only in the lower energy domain ($p_\mu < 10\, GeV$), which corresponds to 99.4% of cosmic μ, which is good enough for the sole purpose of approximation with smaller object. At higher energy, the spectrum is better fit with [15]

$$\frac{dN_\mu}{dp_\mu}(p\mu, \theta = 0^\circ) \approx 0.14 p_\mu^{-2.7} \left(\frac{1}{1 + \frac{1.1 p_\mu}{115}} + \frac{0.054}{1 + \frac{1.1 p_\mu}{850}} \right). \tag{18}$$

The difference between the model and the simulation might be due to the following reasons

1. Cosmic μ with different zenith angle $\theta \neq 0^\circ$ has not been considered in the model
2. Approximation of a constant energy deposit has been adopted (11), while in reality, the energy dissipated inside material of muon should follow a Landau distribution

$$f(x) = \frac{1}{\pi c} \int_0^\infty e^{-t} \cos\left[t \left(\frac{x - \mu}{c} \right) + \frac{2t}{\pi} \log\left(\frac{t}{c} \right) \right] dt \tag{19}$$

   with μ being the location parameter and c being the scale parameter.
3. Lack of implementation of MCS into the theoretical interaction
4. Higher number of events in Monte Carlo simulation might be necessary to produce more accurate result at high energy

Nevertheless, bringing these two factors into the model will greatly increase the accuracy as well as the complexity of the system and thus, further improvements are needed for a good calculation procedure. Meanwhile, for the experiment, the most important improvement is to develop an algorithm of data processing to extract the measurement result in the form of 2-dimensional array, which will inevitably involve taking MCS into account. The dark count rate measurement can also be improved in accuracy by increasing the time interval of each sample taken since an interval of $2s$ is highly susceptible to measurement error.

Due to exploiting natural source of muon, this technique has high potential to develop in the future for various applications, ranging from exploring caves, metal and mineral to scanning vehicles for nuclear weapon as in the simulation at figure 15 since it depends only on the amount of material in between.

6 Conclusion

In this study, our team has been able to

- Learn about cosmic μ and how it interacts with materials

- Deduce a general method to roughly estimate the amount of μ passing through materials and the scanning result for any geometries (MCS neglected and only vertical μ is considered)
- Simulate the radiography results for different more complex geometries
- Work with particle detectors (MPPC and Plastic Scintillator), investigate their characteristics and how they respond to cosmic μ

The study is still incomplete and needs many modifications to be more useful in the future

- Include MCS and cosmic μ angular distribution to the system
- Developing to cosmic μ tomography

7 Project Management

The progress of the group is summarized in the Table 2

Table 2: Project tasks and team progress.

Task	**Done**	**Reasons for differences**
Learn how cosmic μ is created and how it interacts with matters	✓	
Learn how to use G4beamline for particle simulation	✓	
Deduce a mathematical expression/model for cosmic μ spectrum at sea-level	✓	
Deduce a method to estimate muon radiography result theoretically from an assumed geometry and material of a target	✓	
Simulate practical geometries/objects using G4beamline	✓	
Learning about plastic scintillators, MPPC and their characteristics	✓	
Measure cosmic μ using MPPC and plastic scintillators	✓	
Building a prototype μ counter using scintillators and MPPC		Lack of time (only 1 weeks of working with the hardwares were available in Quy Nhon, the first week were used to learn about the components themselves) and equipment (a large amount of scintillators are needed)
Build a cloud chamber		The device was later found to be unsuitable for this application and is thus excluded from this project. However, we are trying to find enough funding from the USTH 20 program to be able to build one.

References

[1] Kunihiro Morishima et al. Discovery of a big void in Khufu's Pyramid by observation of cosmic-ray muons. *Nature*, 552(7685):386–390, 2017.

[2] P.A. Zyla et al. Review of Particle Physics. *PTEP*, 2020(8):083C01, 2020.

[3] R Bellotti, F Cafagna, M Circella, G De Cataldo, CN De Marzo, N Giglietto, P Spinelli, RL Golden, SA Stephens, SJ Stochaj, et al. Measurement of the negative muon spectrum between 0.3 and 40 gev/c in the atmosphere. *Physical Review D*, 53(1):35, 1996.

[4] R Bellotti, F Cafagna, M Circella, CN De Marzo, RL Golden, SJ Stochaj, MP De Pascale, A Morselli, P Picozza, SA Stephens, et al. Balloon measurements of cosmic ray muon spectra in the atmosphere along with those of primary protons and helium nuclei over midlatitude. *Physical Review D*, 60(5):052002, 1999.

[5] M Boezio, P Carlson, T Francke, N Weber, M Suffert, M Hof, W Menn, M Simon, SA Stephens, R Bellotti, et al. Measurement of the flux of atmospheric muons with the caprice94 apparatus. *Physical Review D*, 62(3):032007, 2000.

[6] M Boezio, V Bonvicini, Paolo Schiavon, A Vacchi, N Zampa, D Bergström, P Carlson, T Francke, P Hansen, E Mocchiutti, et al. Energy spectra of atmospheric muons measured with the caprice98 balloon experiment. *Physical Review D*, 67(7):072003, 2003.

[7] S Coutu, JJ Beatty, MA DuVernois, SW Barwick, E Schneider, A Bhattacharyya, CR Bower, JA Musser, A Labrador, D Müller, et al. Energy spectra, altitude profiles, and charge ratios of atmospheric muons. *Physical Review D*, 62(3):032001, 2000.

[8] Sadakazu Haino, T Sanuki, K Abe, K Anraku, Y Asaoka, H Fuke, M Imori, A Itasaki, T Maeno, Y Makida, et al. Measurements of primary and atmospheric cosmic-ray spectra with the bess-tev spectrometer. *Physics Letters B*, 594(1-2):35–46, 2004.

[9] CERN. Geant4 material database. https://geant4-userdoc.web.cern.ch/UsersGuides/ForApplicationDeveloper/html/Appendix/materialNames.html.

[10] Tom Roberts. G4beamline user's guide. *Muons, Inc*, pages 3468–3470, 2013.

[11] Sea Agostinelli, John Allison, K al Amako, John Apostolakis, H Araujo, P Arce, M Asai, D Axen, S Banerjee, G 2 Barrand, et al. Geant4—a simulation toolkit. *Nuclear instruments and methods in physics research section A: Accelerators, Spectrometers, Detectors and Associated Equipment*, 506(3):250–303, 2003.

[12] John Allison, Katsuya Amako, JEA Apostolakis, HAAH Araujo, P Arce Dubois, MAAM Asai, GABG Barrand, RACR Capra, SACS Chauvie, RACR Chytracek, et al. Geant4 developments and applications. *IEEE Transactions on nuclear science*, 53(1):270–278, 2006.

[13] J Allison, Katsuya Amako, John Apostolakis, Pedro Arce, M Asai, T Aso, E Bagli, A Bagulya, S Banerjee, GJNI Barrand, et al. Recent developments in geant4. *Nuclear Instruments and Methods in Physics Research Section A: Accelerators, Spectrometers, Detectors and Associated Equipment*, 835:186–225, 2016.

[14] K. Sato A. Ghassemi and K. Kobayashi. MPPC, ed. by Y. Ohashi, Y. Enomoto,and Y. Adachi, HAMAMATSU PHOTONICS K. K. *Solid State Division*, Japan,2017.

[15] Thomas K Gaisser, Ralph Engel, and Elisa Resconi. *Cosmic rays and particle physics*. Cambridge University Press, 2016.